Applied Geochemistry 24 (2009) 504–516

Contents lists available at ScienceDirect

Applied Geochemistry

journal homepage: www.elsevier.com/locate/apgeochem

Relationship between CO_2-dominated fluids, hydrothermal alterations and gold mineralization in the Red Lake greenstone belt, Canada

Guoxiang Chi [a,*], Yongxing Liu [a], Benoît Dubé [b]

[a] Department of Geology, University of Regina, Regina, SK, Canada S4S 0A2
[b] Geological Survey of Canada, 490 rue de la Couronne, Quebec, Canada G1K 9A9

ARTICLE INFO

Article history:
Available online 16 December 2008

ABSTRACT

The Red Lake greenstone belt is one of the foremost Au mining camps in Canada and hosts the world-class Campbell-Red Lake Au deposit. Belt-scale hydrothermal alteration is characterized by proximal ferroan dolomite zones associated with Au mineralization surrounded by distal calcite zones, both being accompanied by potassic alterations (sericite, muscovite, and biotite). At the Campbell-Red Lake and Cochenour deposits Au mineralization (in particular high-grade ore) is associated with silica and sulfides (especially arsenopyrite) that replace carbonate ± quartz veins and the host rocks. The prevalence of carbonic fluid inclusions and rare occurrence of aqueous-bearing inclusions in carbonate–quartz–Au veins in the Campbell-Red Lake deposit, and the consistency of homogenization temperatures of carbonic inclusions within individual fluid inclusion assemblages (FIA), have been interpreted to indicate that H_2O-poor, CO_2-dominated fluids were responsible for the carbonate veining and Au mineralization. Further studies of fluid inclusions in carbonate–quartz veins within and outside the deformation zone hosting the Campbell-Red Lake deposit (the Red Lake Mine trend) including the Cochenour Au deposit, the Redcon Au prospect, and outcrops in the distal calcite zone also reveal the dominance of carbonic fluid inclusions in vein minerals. These studies indicate that CO_2-dominated fluids were flowing through fractures during carbonate vein formation and Au mineralization both within and outside major structures. The carbonic fluid may have been initially undersaturated with water, or it may have resulted from phase separation of an H_2O–CO_2–NaCl fluid. In the latter case, phase separation modeling indicates that the initial fluid likely had X_{CO_2} values larger than 0.8. Calculations based on hydrothermal mineral assemblages indicate X_{CO_2} values in the host rocks from 0.025 to 0.85, reflecting a change from CO_2-dominated fluids in the fractures (veins) to H_2O-dominated fluids in the host rocks away from the fractures. The CO_2-dominated fluids were likely advected from granulite facies in the deeper crust, whereas the H_2O-dominated fluids were derived from the ambient host rocks of amphibole to greenschist facies. Calculations based on CO_2 requirements and source constraints indicate that the mineralizing fluids were likely two orders of magnitude more enriched in Au than the commonly assumed values of a few μg/L, which may explain why the Campbell-Red Lake deposit has a very high-grade of Au (average 21 g/t for the whole deposit and 81 g/t for the Goldcorp High-Grade zone). Fluid inclusion data suggest that the carbonate veining and Au mineralization likely took place at depths from 7 to 14 km. The development of crustiform–colloform structures in the carbonate ± quartz veins, which was previously interpreted to indicate relatively shallow environments, may alternatively have been related to extremely high fluid pressures and the CO_2-dominated nature of the fluids, which could have enhanced the brittle properties of the rocks due to their high wetting angles.

1. Introduction

It is well known that Au deposits formed in metamorphic terranes (Groves et al., 2003; Goldfarb et al., 2005), including orogenic Au deposits (Groves et al., 1998) or greenstone-hosted quartz–carbonate vein-type Au deposits (Poulsen et al., 2000; Dubé and Gosselin, 2007), and intrusion-related Au deposits (Lang and Baker, 2001), are commonly associated with CO_2-enriched, low-salinity fluids as recorded by fluid inclusions (Ridley and Diamond, 2000; Baker, 2002). According to Ridley and Diamond (2000), the CO_2 mole fraction of the ore-forming fluids ranges from 0.05 to 0.90, but the most frequently recorded values are in the range from 0.10 to 0.25, indicating H_2O-dominated fluid systems. However, in some deposits, including the world-class Ashanti Au belt (Ghana) and Campbell-Red Lake Au deposit (Canada), fluid inclusion studies suggest that the ore-forming fluids were dominated by CO_2 (Schmidt Mumm et al., 1997, 1998; Chi et al., 2006). In these

* Corresponding author.
E-mail address: guoxiang.chi@uregina.ca (G. Chi).

0883-2927/$ - see front matter © 2008 Elsevier Ltd. All rights reserved.
doi:10.1016/j.apgeochem.2008.12.005

and a few other examples, e.g., the Bin Yauri Au deposit in Nigeria (Garba and Akande, 1992) and the Fazenda Maria Preta Au deposit in Brazil (Xavier and Foster, 1999), carbonic fluid inclusions without a visible aqueous phase are almost the only type of inclusions present. Although carbonic inclusions may be produced by fluid phase separation (e.g., Robert and Kelly, 1987; Guha et al., 1991) and/or preferential leakage of H_2O relative to the carbonic components after entrapment (Hollister, 1988, 1990; Bakker and Jansen, 1994; Johnson and Hollister, 1995), these mechanisms cannot satisfactorily explain why so few aqueous inclusions were entrapped and/or preserved in these cases, and so the predominance of carbonic fluid inclusions is interpreted to reflect a CO_2-dominated fluid system (Schmidt Mumm et al., 1997, 1998; Chi et al., 2006). It remains unclear, however, how such fluids originated and were distributed in the greenstone belts, and how they are related to Au mineralization and hydrothermal alteration including hydrous mineral assemblages (Klemd, 1998; Ridley and Diamond, 2000; Goldfarb et al., 2005). These questions are examined in this paper for the Archean Red Lake greenstone belt, Canada, where the predominance of carbonic fluid inclusions has been reported for the Campbell-Red Lake deposit (Tarnocai, 2000; Chi et al., 2002, 2003, 2006).

The Red Lake greenstone belt in western Ontario is one of Canada's foremost Au mining districts, with 105 Au showings/deposits within a small area of about 500 km^2 (Fig. 1; Sanborn-Barrie et al., 2004). The total production plus remaining reserve and resources is nearly 1000 t of Au, of which 840 t is from the Campbell-Red Lake Au deposit (Chi et al., 2006, in written communication from S. McGibbon in 2005) and about 150 t Au from the remaining deposits (Lichtblau and Storey, 2005). The Campbell-Red Lake deposit has been interpreted as a metamorphosed epithermal deposit (Penczak and Mason, 1997, 1999), but several other studies (e.g., MacGeehan et al., 1982; Mathieson and Hodgson, 1984; Andrews et al., 1986; Tarnocai et al., 1997; Menard and Pattison, 1998; Tarnocai, 2000; Parker, 2000; Thompson, 2003; Dubé et al., 2004) indicate a broadly contemporaneous relationship between the mineralization, regional deformation, magmatic intrusion and metamorphism (i.e., syn-orogeny). Also the geological setting as well as structural and alteration features shares similarities to those of orogenic Au deposits (Groves et al., 1998). However, unlike most greenstone-hosted orogenic Au deposits where carbonate contents in the veins are less than 5–15 vol.% (Goldfarb et al., 2005), carbonate constitutes the original main components of Au-bearing carbonate ± quartz veins in the Campbell-Red Lake Au deposit. The abundance of carbonate alteration throughout the greenstone belt, and the unusually well developed carbonate ± quartz veins with which Au mineralization is commonly associated spatially, have been noticed by many authors (e.g., Andrews et al., 1986; Parker, 2000; Poulsen et al., 2000; Dubé et al., 2003), but the relationship between the carbonate alteration/veining and the newly recognized CO_2-dominated fluids (Chi et al., 2006), and the apparent conflict between the development of hydrous alteration and the H_2O-poor nature of the CO_2-dominated fluids, has never been examined.

This paper summarizes the evidence for CO_2-dominated fluids in the Campbell-Red Lake Au deposit (Tarnocai, 2000; Chi et al.,

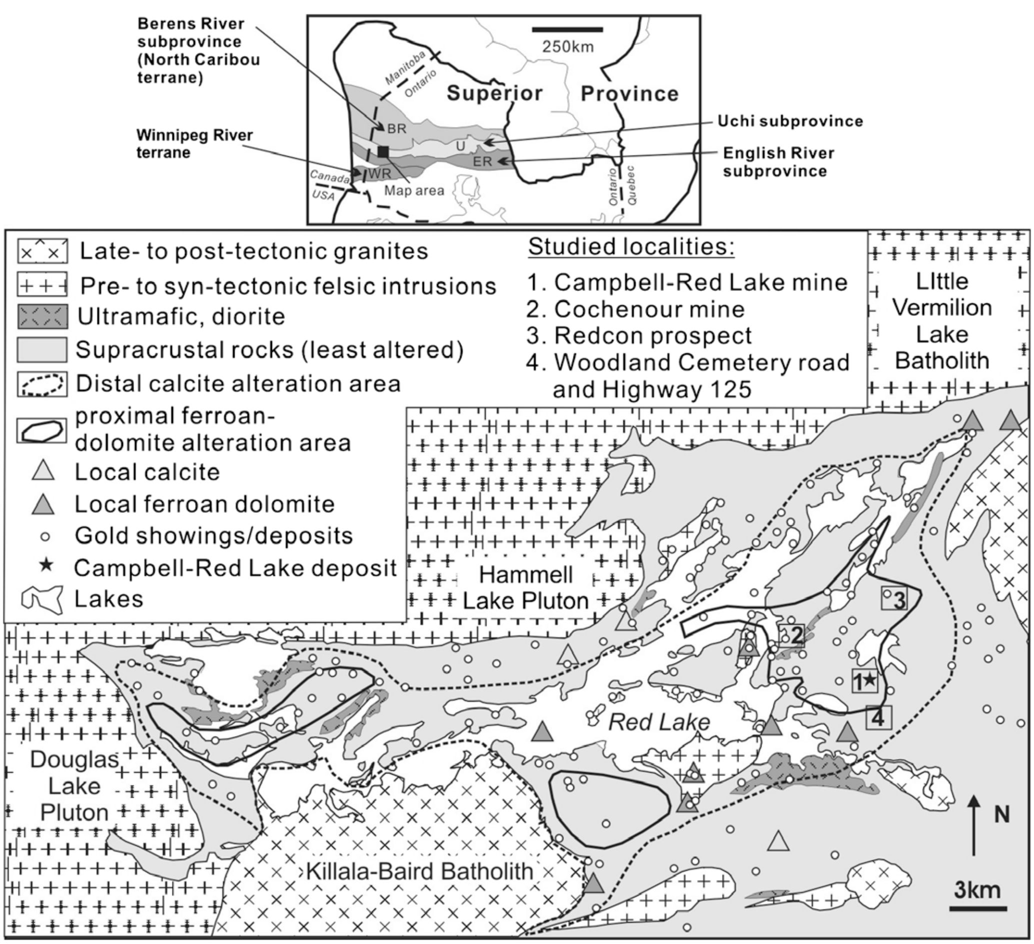

Fig. 1. Geological map of the Red Lake greenstone belt showing the distribution of Au deposits/occurrences, carbonate alterations, and localities studied (after Sanborn-Barrie et al., 2004).

2002, 2003, 2006) and provides new evidence indicating that such fluids were also present outside the deformation zone hosting the Campbell-Red Lake deposit. Based on pressure–temperature conditions estimated from metamorphic mineral assemblages and fluid inclusion microthermometry data, fluid phase separation modeling is used to constrain the minimum X_{CO_2} of the initial CO_2-dominated fluids. Calculations of the total amount of CO_2 input from auriferous hydrothermal fluids are then carried out following a similar approach to Phillips et al. (1987) for the Golden Mile Au deposit (Kalgoorlie, Australia) to provide compositional constraints on Au solubility and source regions of the CO_2-dominated fluids in the Red Lake greenstone belt. Finally, the relationship between CO_2-dominated fluids and hydrous alteration, the mechanisms of carbonate deposition in the veins, the nature of the spatial association between Au mineralization and carbonate ± quartz veins, the capacity of the CO_2-dominated fluids to carry Au, and the apparent discrepancy between colloform–crustiform structures of the carbonate ± quartz veins and deep hydrothermal environments indicated by fluid inclusions and metamorphic mineral assemblages, are discussed.

2. Geological setting

The Red Lake greenstone belt is part of the Uchi subprovince of the Superior province. It consists of Mesoarchean (2990–2890 Ma) and Neoarchean (2750–2730 Ma) volcanic-dominated rocks (Sanborn-Barrie et al., 2004 and references therein). The Mesoarchean comprises mafic-ultramafic volcanic rocks of the Balmer assemblage (2990–2960 Ma), intermediate to felsic calc-alkaline flows and pyroclastic rocks of the Ball assemblage (2940–2920 Ma), and intermediate calc-alkaline pyroclastic rocks overlain by clastic sedimentary rocks and banded iron-formation of the Bruce Channel assemblage (Dubé et al., 2004; Sanborn-Barrie et al., 2004 and references therein). The Neoarchean rocks, separated by a regional unconformity from the Mesoarchean, consist of calc-alkaline and tholeiitic volcanic and volcaniclastic rocks of the Confederation assemblage (2750–2730 Ma), polymictic conglomerate and finer clastic sedimentary rocks of the Huston assemblage, and calc-alkaline rocks of the Graves assemblage (ca. 2732 Ma) (Dubé et al., 2004; Sanborn-Barrie et al., 2004 and references therein).

The supracrustal assemblages were affected by two main episodes of penetrative deformation: D1 is related to a W–E shortening stress regime from ca. 2742 to 2733 Ma, whereas D2 reflects N–S shortening related to the Uchian phase of the Kenoran orogeny between ca. 2723 and 2712 Ma, which is related to the collision between the North Caribou terrane to the north of the Red Lake greenstone belt and the Winnipeg River terrane to the south (Sanborn-Barrie et al., 2004). More recently, Percival et al. (2006) indicated that this large scale collisional event (Uchian orogeny) occurred from ~2.72 to 2.70 Ga. Post-collisional deformation (D3) is locally recorded and its age is constrained to be after ca. 2700 Ma (Menard et al., 1999; Dubé et al., 2004).

The supracrustal rocks were intruded by granitoids of various ages (Fig. 1), including the Douglas Lake pluton (2734 Ma), Little Vermilion Lake batholith (2731 Ma), Hammell Lake pluton (2717 Ma), Dome stock (2718 Ma), Killala-Baird batholith (2704 Ma), and Cat Island pluton (2697–2699 Ma) (Corfu and Andrews, 1987; Dubé et al., 2004; Sanborn-Barrie et al., 2004). Felsic-intermediate dykes of 2714–2696 Ma and lamprophyre dykes of 2702–2699 Ma are present (Dubé et al., 2004). The granitoids are classified by Thompson (2003) into 3 groups: (1) pre-orogenic (>2730 Ma), (2) early syn-orogenic (2720–2717 Ma), and (3) late syn-orogenic (2704–2699 Ma).

The volcanic and sedimentary rocks and the early granitoid rocks were metamorphosed to greenschist-to-amphibole facies (Sanborn-Barrie et al., 2004, and references therein). Metamorphic grade increases from greenschist facies in the middle of the greenstone belt to amphibole facies at the margin of the belt, which is surrounded by granitoid intrusions, and the boundaries between metamorphic zones (isograds) are broadly parallel to the contact between the supracrustal rocks and the granitoid rocks (Andrews et al., 1986; Damer, 1997; Thompson, 2003). This metamorphic pattern has been interpreted by many (Andrews et al., 1986; Damer, 1997; Menard and Pattison, 1998; Tarnocai, 2000) as indicating contact metamorphism. However, Thompson (2003) pointed out that some of the granitoid intrusions are too young or too old to be the heat source for regional metamorphism, which peaked during the major phase of the orogeny, and petrographic evidence indicates that the main phase of metamorphism overlapped with ductile deformation associated with crustal shortening and thickening. Therefore, although granitoid intrusions likely caused localized contact metamorphism, which overprinted regional metamorphism, the metamorphic pattern of the Red Lake greenstone belt mainly reflects the results of peak regional metamorphism during D2 (Thompson, 2003). In other words, both granitoids and regional metamorphism are products of crustal shortening and thickening, with granitoid intrusions outlasting peak metamorphism.

Gold deposits, mostly hosted in the Balmer assemblage, occur along major deformation zones (Andrews et al., 1986) and are commonly spatially associated with carbonate ± quartz veins. However, besides the Campbell-Red Lake and Cochenour Au deposits, there are other styles of Au mineralization in Red Lake as illustrated by the amphibolite-facies, disseminated-replacement-style Au mineralization at Madsen, the second largest deposit in the district (Dubé et al., 2000) or the quartz–tourmaline Au-bearing veins as typified by the Buffalo mine. The Campbell-Red Lake deposit, by far the largest deposit in the district, is characterized by numerous barren to low grade colloform–crustiform, cavity-filling carbonate ± quartz veins overprinted by auriferous silicification (MacGeehan and Hodgson, 1982; Penczak and Mason, 1997, 1999; Tarnocai, 2000; Twomey and McGibbon, 2001; Dubé et al., 2001, 2002, 2004). As indicated in Dubé et al. (2004), five different styles of Au mineralization are present in the Campbell-Red Lake deposit: (1) sulfide-rich veins and replacement-style ore, mainly present at the Red Lake mine and spatially associated with the Dickenson and the Campbell faults, (2) carbonate ± quartz veins, better developed in the upper portion of the deposit at the Campbell mine, (3) magnetite-rich ore, (4) high-grade arsenopyrite-rich silicification characterized by multi-ounce ore zones that typify the Goldcorp High-Grade zone, and (5) abundant visible Au coating and filling late fractures. The Goldcorp High-Grade zone of the Campbell-Red lake deposit is the best example of styles 3, 4 and 5 (Dubé et al., 2004). The timing of Au mineralization has been controversial. The colloform–crustiform and cockade structures that are well developed in the carbonate ± quartz veins led Penczak and Mason (1997, 1999) to interpret the carbonate veining and mineralization as pre-penetrative deformation and pre-regional metamorphism events, and assigned the Campbell-Red Lake Au deposit to a deformed and metamorphosed low-sulfidation epithermal type. Several authors (e.g., MacGeehan et al., 1982; Mathieson and Hodgson, 1984; Andrews et al., 1986; Tarnocai et al., 1997; Menard and Pattison, 1998; Tarnocai, 2000; Parker, 2000; Twomey and McGibbon, 2001; Thompson, 2003; Dubé et al., 2004), however, consider Au mineralization as broadly syn-deformation and syn-metamorphic, although the interpretation of the age(s) of peak metamorphism is different for different authors. Based on their study of the Goldcorp High-Grade zone at the Red Lake mine of the Campbell-Red lake deposit, Dubé et al. (2004) constrained the age of the high-grade Au mineralization to be mainly between 2723 and 2712 Ma, an interval similar to those proposed by Corfu and Andrews (1987) and Penczak and Mason (1997) for the entire Campbell-Red Lake deposit. This age interval is also in the same range as the main phase metamorphism and deformation defined by Thompson (2003), and broadly coincides with the Uchian orogeny (Sanborn-Barrie et al., 2004; Percival et al., 2006). Minor mineralization took place after 2702 Ma, probably related to D3 (Menard et al., 1999; Dubé et al., 2004).

The Red Lake greenstone belt has experienced extensive hydrothermal alteration, most noticeably carbonate alteration. Parker (2000) divided carbonate alteration into two types, i.e., "proximal ferroan dolomite alteration", where major Au deposits occur, and "distal calcite alteration", where only minor Au occurrences are found (Fig. 1). Conflicting crosscutting relationships between calcite and ferroan dolomite veins in the boundary zone between the two types of carbonate alteration suggests that they are broadly contemporaneous (Parker, 2000). Besides carbonatization, potassic alteration is also widespread in the Red Lake greenstone belt (Andrews et al., 1986; Parker, 2000). The potassic alteration in the distal calcite zones is characterized by sericitization, whereas that in the proximal ferroan dolomite zones consists of sericite/muscovite/fuchsite and some biotite in the greenschist facies, and pervasive biotite + muscovite in amphibolite-facies (Parker, 2000). At the vein or replacement ore scale in the Goldcorp High-Grade zone of the Red Lake mine, Au-bearing silicified carbonate ± quartz veins are commonly surrounded by a centimeter- to meter-wide reddish-brown biotite–carbonate alteration envelope, and by an outer, meter-wide, garnet–chlorite–magnetite assemblage (Damer, 1997; Twomey and McGibbon, 2001; Dubé et al., 2004; Cadieux et al., 2006, and references therein) locally associated with centimeter- to meter-wide barren "bleached zone" containing andalusite-muscovite-quartz-ilmenite in the ampibolite facies domains (Tarnocai, 2000; Twomey and McGibbon, 2001; Dubé et al., 2002, 2004; Cadieux et al., 2006). In the Campbell-Red Lake deposit, the aluminous bleached zones are common in variolitic pillowed flows and represent an early pre-mineralization assemblage (Penczak and Mason, 1999; Tarnocai, 2000; Dubé et al., 2004; Cadieux et al., 2006). Cadieux et al. (2006) indicated that in the Goldcorp High-Grade zone the aluminous assemblage is pre-colloform carbonate ± quartz veins and has no clear spatial relationship with the high-grade ore. Such aluminous alteration is compatible with metamorphosed argillic and advanced argillic alteration due to acid leaching by low pH fluids (Penczak and Mason, 1997; Cadieux et al., 2006). In the Goldcorp High-Grade zone, Au mineralization is clearly related to silica and arsenopyrite replacement of carbonate ± quartz veins and the host rocks (Dubé et al., 2002, 2004), but reddish-brown biotite–carbonate alteration is also considered to be related at least spatially to the auriferous hydrothermal system (Twomey and McGibbon, 2001; Dubé et al., 2002, 2004). However, biotite–carbonate alteration is also found where there is no silica-arsenopyrite replacement and Au mineralization (Cadieux et al., 2006), and auriferous silica and arsenopyrite alteration is seen replacing biotite–carbonate alteration (Dubé et al., 2002; Parker, 2000). Biotitic alteration in amphibolite-facies metavolcanic rocks may also contain variable amounts of aluminosilicate minerals such as andalusite, staurolite and cordierite, which have been interpreted to have formed from metamorphism of previously altered rocks (Penczak and Mason, 1999; Parker, 2000).

3. CO_2-dominated fluid inclusions in the Red Lake greenstone belt

The development of extensive carbonate alteration in the Red Lake greenstone belt, as outlined above, does not necessarily indicate involvement of CO_2-dominated fluids. The evidence for CO_2-dominated fluids comes mainly from fluid inclusions entrapped in hydrothermal vein minerals, particularly the predominance of carbonic fluid inclusions without a visible aqueous phase and the rarity of aqueous inclusions, as observed in the Campbell-Red Lake deposit (Chi et al., 2003, 2006). Similar observations are made in this study for three other occurrences (Cochenour, Redcon, and Sandy Bay – Woodland Cemetery outcrops) with different local geological setting in the eastern part of the Red Lake greenstone belt (Fig. 1). These observations are summarized in Table 1 and described below. Fluid inclusions randomly distributed in three dimensions and occurring in isolation and clusters are interpreted as primary or pseudosecondary inclusions. All the fluid inclusions studied are considered to be primary or pseudosecondary unless otherwise indicated (labelled "s" in Table 1).

The Campbell-Red Lake Au deposit is located in a SE-trending hydrothermal/structural corridor known as the Red Lake Mine trend (Dubé et al., 2003, 2004, and references therein). The deposit, located within the proximal ferroan dolomite alteration zone of Parker (2000), is characterized by numerous barren to low-grade banded crustiform ankerite ± quartz veins and ankerite-cemented cockade breccias, which are replaced and overprinted by quartz and associated sulfides (mainly arsenopyrite) and native Au. In the Goldcorp High-Grade zone, the Au-bearing silicified carbonate ± quartz veins are commonly surrounded by a biotite–carbonate alteration envelope (Fig. 2A) (Twomey and McGibbon, 2001; Dubé et al., 2004; Cadieux et al., 2006, and references therein). The host rocks were metamorphosed to greenschist–amphibole facies (transition zone) (Thompson, 2003). Fluid inclusions in ankerite and associated quartz (Q1) as well as in quartz associated with Au (Q2) are predominantly carbonic, while aqueous and aqueous-carbonic inclusions are rare, and bulk analysis of fluid inclusions by gas chromatography indicates negligible H_2O (Chi et al., 2006). However, aqueous and aqueous-carbonic inclusions are common in post-mineralization calcite and quartz (Q3) (Chi et al., 2003). The aqueous inclusions studied in Q1, Q2, and Q3 are isolated, scattered and clustered, and are considered as primary and pseudosecondary as are carbonic inclusions, although the co-entrapment of carbonic inclusions and aqueous inclusions has not been shown by fluid inclusion assemblages (Chi et al., 2002, 2003, 2006). Homogenization temperatures of carbonic inclusions range from −2.4 to +30.6 °C (to liquid) for ankerite and +0.3 to +26.5 °C for Au-related quartz (Table 1). Despite these overall wide ranges, homogenization temperatures within individual fluid inclusion assemblages (FIA) are consistent, arguing against post-entrapment modification (preferential H_2O leakage) as the mechanism of formation of carbonic inclusions (Chi et al., 2006). Homogenization temperatures of aqueous inclusions range from 171 to 344 °C, 252–380 °C, and 73–326 °C for ankerite, auriferous quartz and post-ore quartz and calcite, respectively (Table 1).

The Cochenour Au deposit is hosted by the same deformation zone as the Campbell-Red Lake deposit (i.e., the Red Lake Mine trend) and located within the greenschist–amphibole transition zone (Thompson, 2003) and the proximal ferroan dolomite alteration zone (Parker, 2000). It is characterized by extensive carbonate ± quartz veining (Fig. 2B) overprinted, at least in part, by silicification, sulfide replacement, and Au mineralization (Dubé et al., 2003, and references therein). Fluid inclusions are predominantly carbonic in ankerite and associated coarsely crystalline quartz (Q1) and in Au-associated fine-grained quartz (Q2). Aqueous and aqueous-carbonic inclusions are generally rare, but can be locally common in some of the quartz associated with ankerite (Q1). Homogenization temperatures of carbonic inclusions range from −12.6 to +20.5 °C (to liquid) for ankerite and −0.2 to +20.5 °C for Au-related quartz (Table 1). Homogenization temperatures of aqueous inclusions in quartz associated with ankerite range from 110 to 265 °C (Table 1).

Table 1
Characteristics of fluid inclusions from four different deposits/occurrences in eastern Red Lake greenstone belt[a].

Localities	Campbell-Red Lake deposit			Cochenour deposit		Redcon prospect		Sandy Bay–Woodland Cemetery
Deformation zone	Red Lake Mine trend			Red Lake Mine trend		Low-strain zone		Low-strain zone
Metamorphic grade	Greenschist–amphibole transition			Greenschist–amphibole transition		Greenschist–amphibole transition		Greenschist
Alteration zone	Proximal ankerite			Proximal ankerite		Proximal ankerite		Distal calcite
Host mineral	Ank – Q1	Q2 (syn-ore)	Cal3-Q3	Ank – Q1	Q2 (syn-ore)	Ank	Q2 (syn-ore)	Q-D
Carb FI	+++++	+++++	+++	+++++	+++++	+++++	+++++	+++
Aq-Carb FI	–	–	+	+	–	–	+ (s)	+ (s)
Aq FI	–	–	+	+	–	–	+ (s)	+ (s)
T_h of Carb FI	−2.4 to +30.6 (L)	+0.3 to +26.5 (L)	+14.2 to 26.8 (L)	−12.6 to +20.5 (L)	−0.2 to +20.5 (L)	+2.0 to +26.5 (L)	−25.0 to +31.0 (L)	−18.5 to −11.8 (L)
T_h of Aq FI	171–344	252–380	73–326	110–265			235 to >255	286–384

Carb = carbonic; FI = fluid inclusions; Aq = aqueous; T_h = homogenization temperatures (°C); Ank = ankerite; Q1 = quartz associated with ankerite; Q2 = quartz post-dating ankerite and associated with gold mineralization; Cal 3 = calcite (post-mineralization); Q3 = quartz post-dating mineralization and associated with calcite; Q–D = quartz (distal zone); "+++++" = predominant; "+++" = abundant; "+" = common; "–" = rare; "+ (s)" = common as secondary inclusions.
[a] Data for the Campbell-Red Lake deposit are from Chi et al. (2002, 2003, 2006); others are from this study.

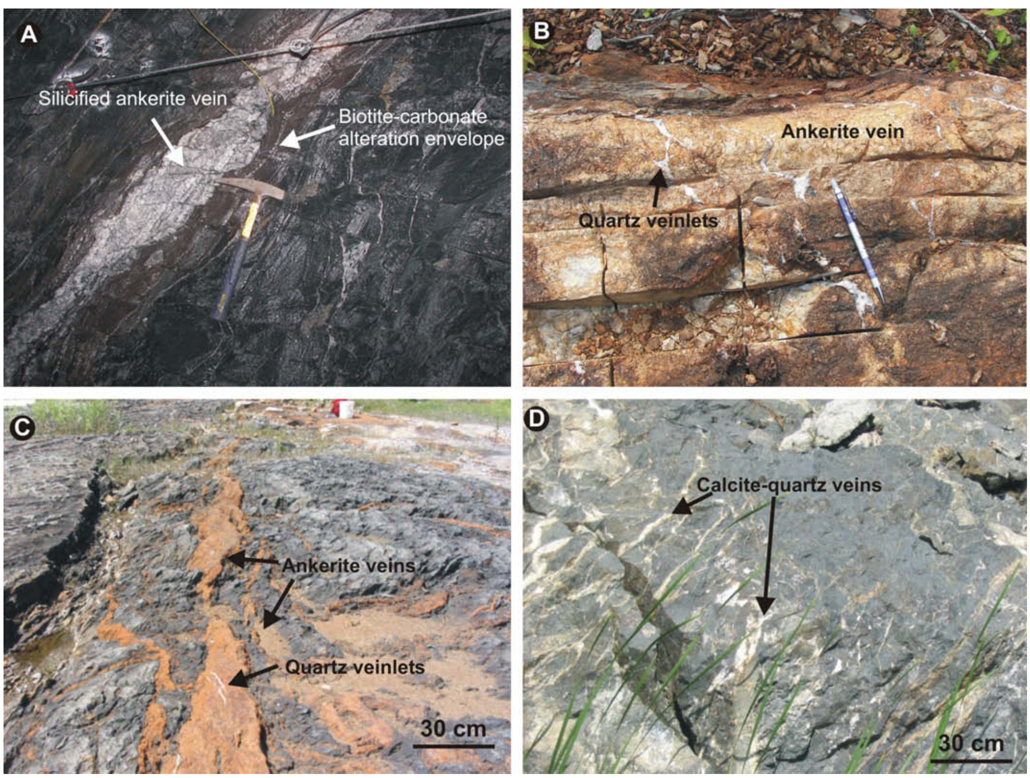

Fig. 2. Photographs showing the occurrences of carbonate–quartz veins in different localities in eastern Red Lake greenstone belt: (A) a crustiform ankerite vein with silicification and Au mineralization, surrounded by a biotite–carbonate alteration envelope, from the Red Lake mine; (B) an ankerite vein with crustiform structures cut by minor quartz veinlets, Cochenour deposit; (C) an ankerite vein (rusted) crosscut by minor quartz veinlets (white), Redcon prospect; (D) calcite–quartz veins in the distal calcite zone, outcrop near the intersection of the Sandy Bay Road and Highway 125.

The Redcon Au prospect is situated about 4 km NE of the Red Lake Mine trend, in an area of relatively weak deformation. It is located within the transition zone between greenschist and amphibole facies (Thompson, 2003) and the proximal ferroan dolomite alteration zone (Parker, 2000). A 1–2 m wide ankerite vein cuts weak foliations, and is in turn cut by quartz-actinolite stringers associated with Au (Fig. 2C). Fluid inclusions in ankerite and quartz (Q2) are predominantly carbonic, with homogenization temperatures ranging from +2.0 to +26.5 °C and from −25.0 to +31.0 °C (to liquid), respectively (Table 1). Homogenization temperatures of isolated carbonic inclusions are similar within individual quartz grains (Fig. 3A), and fall in a very small range within individual healed fractures (Fig. 3B), supporting a non-H_2O leakage origin of the carbonic inclusions. Aqueous and aqueous-carbonic inclusions are common in healed fractures, likely of secondary origin, and have homogenization temperatures from 235 to >255 °C (Table 1).

The outcrops near the intersections of the Sandy Bay and Woodland Cemetery roads with Highway 125 are situated less than 3 km south of the Red Lake Mine trend. The host rocks are within the greenschist facies (Thompson, 2003) and the distal calcite alteration zone (Parker, 2000). Centimeter-scale calcite-quartz veins occur in relatively low-strained volcanic rocks (Fig. 2D). Fluid inclusions are generally less developed than in other occurrences. Carbonic inclusions are abundant in quartz associated with calcite

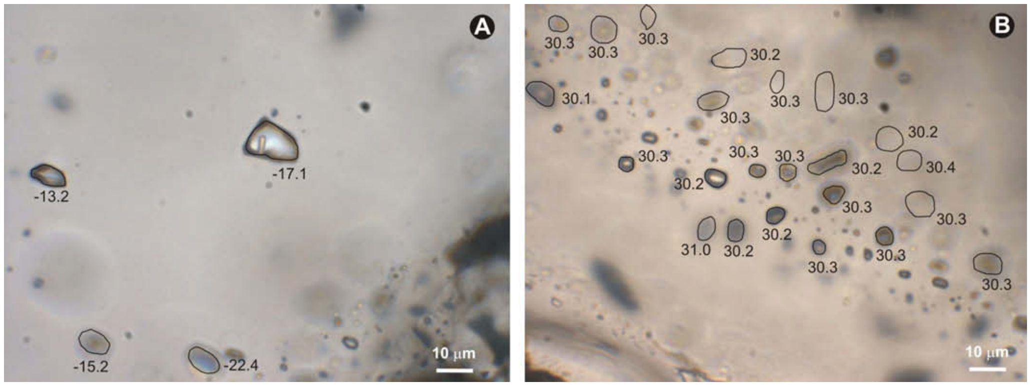

Fig. 3. (A) Relatively isolated carbonic fluid inclusions in quartz, Redcon prospect. The homogenization temperatures (to liquid) are not significantly different between the individual inclusions. (B) Carbonic fluid inclusions in a healed fracture in quartz, Redcon prospect. Homogenization temperatures fall in a small range, mainly from +30.1 to +30.4 (to liquid).

and show homogenization temperatures from −18.5 to −11.8 °C (Table 1). Aqueous and aqueous-carbonic inclusions commonly occur in healed fractures, possibly as secondary inclusions, and have homogenization temperatures from 286 to 384 °C (Table 1).

In summary, carbonic inclusions without a visible aqueous phase are predominant in the Campbell-Red Lake and Cochenour deposits and Redcon prospect and abundant in the Sandy Bay – Woodland Cemetery outcrops. The absence of an aqueous phase, even in relatively large and angular carbonic inclusions, together with gas chromatography analyses of bulk fluid inclusions from the Campbell-Red Lake deposit which indicate negligible H_2O (Chi et al., 2006), suggests that the carbonic inclusions are truly very low in water. The fact that the homogenization temperatures of the carbonic inclusions fall in a small range within individual fluid inclusion assemblages indicates that the carbonic inclusions did not result from preferential leakage of H_2O from initially carbonic-aqueous inclusions – such a mechanism would likely have caused different degrees of H_2O leakage depending on the size and shape of individual inclusions, leading to coexistence of fluid inclusions of different CO_2/H_2O ratios and different homogenization temperatures. As shown in the next section, the carbonic inclusions may have been produced by phase separation of an initially carbonic-aqueous fluid, but this initial fluid must be CO_2-dominated as constrained from phase separation modeling. Therefore, the fluid inclusion data indicate that CO_2-dominated fluids were circulating in the fracture systems in the Red Lake greenstone belt during carbonate veining and Au mineralization. These fluids were not only active within major deformation zones (the Red Lake Mine trend), but were present in the less strained areas as well (e.g., the Redcon prospect and Sandy Bay – Woodland Cemetery outcrops). The CO_2-dominated fluids were not limited to the proximal ankerite zone hosting major Au mineralization either, but were also present in the distal calcite zones. However, aqueous components became more important after the main phase of carbonatization and Au mineralization, as reflected by the common occurrences of primary aqueous inclusions in post-mineralization quartz and calcite and secondary aqueous inclusions in other vein minerals.

4. *P–T* conditions and constraints on X_{CO_2} from fluid phase separation modeling

The limited number of aqueous inclusions from the Campbell-Red Lake deposit gives a large range of homogenization temperatures from 171 to 380 °C (Table 1), which are significantly lower than the peak metamorphism temperature (about 450–550 °C) estimated by different authors based on metamorphic mineral assemblages (Table 2). The main phase of Au mineralization in the Red Lake greenstone belt has been limited by isotopic dating to 2723–2712 Ma (Corfu and Andrews, 1987; Penczak and Mason, 1997; Dubé et al., 2004), which coincides with the main phase of regional metamorphism (Thompson, 2003). Textural evidence suggests that auriferous hydrothermal alteration was broadly synchronous with the peak metamorphism at the Campbell mine (Tarnocai et al., 1997; Tarnocai, 2000). The fact that hydrothermal alteration mineral assemblages change systematically with metamorphic grades (Parker, 2000) also suggests that the hydrothermal activities associated with Au mineralization in the Red Lake greenstone belt were broadly contemporaneous with regional peak metamorphism, similar to many orogenic Au deposits (Mikucki and Ridley, 1993; McCuaig and Kerrich, 1998). The reason why the homogenization temperatures of aqueous inclusions are so variable and lower than the peak metamorphism temperatures may be related to pressure fluctuation and physical separation of the aqueous and carbonic phases during trapping of the inclusions (Robert and Kelly, 1987). If an aqueous phase is saturated with the carbonic phase (i.e., the two phases are in physical contact with

Table 2
Pressure–temperature conditions of peak metamorphism and hydrothermal alteration at the Campbell-Red Lake deposit.

Methods and references	Red Lake mine		Campbell mine	
	Pressures (kbar)	Temperatures (°C)	Pressures (kbar)	Temperatures (°C)
Metamorphic mineral assemblage: TWEEQU program (Damer, 1997)	1.4–2.0	435–480		
Metamorphic mineral assemblage: WEBINVEQ program (Damer, 1997)	1.0–2.2	450–550		
Metamorphic mineral assemblage (Mathieson and Hodgson, 1984)	3.8–4.2	520–540		
Arsenopyrite geothermometer (Mathieson and Hodgson, 1984)		500–530		
Metamorphic mineral assemblage (Christie, 1986)			3–4	440–510
Metamorphic mineral assemblage (Tarnocai, 2000)			<3	465–545
Metamorphic mineral assemblage (Thompson, 2003)	2–4 kbar; 500–550 °C for transition from greenschist-to-amphibole facies			
Isochore of carbonic inclusion with homogenization temperature of −2.4 °C (Chi et al., 2003)	2.7–3.6 kbar for temperature range from 350 to 550 °C			

each other) during trapping of the inclusions, the homogenization temperatures should be equal to the trapping temperatures. However, if the two phases are physically separated (e.g., located in separate intracrystal microfractures), a decrease of fluid pressure will purge part of the carbonic component from the aqueous phase, and a later increase of fluid pressure will make the aqueous phase become undersaturated with the carbonic components (Robert and Kelly, 1987). If this aqueous phase is then entrapped (sealed) as inclusions, their homogenization temperatures will be lower than the trapping temperatures, and "pressure corrections" are required to obtain the trapping temperatures. Robert and Kelly (1987) have shown that temperature corrections ranging from 50 to 200 °C may be applicable to the aqueous inclusions in the case of the Sigma Au deposit in the Abitibi greenstone belt. Therefore, depending on the magnitude of fluid pressure fluctuation, the homogenization temperatures can be variably lower than the trapping temperatures, although it is possible that the higher part of the homogenization temperature spectrum may overlap with the trapping temperatures.

Taking into account all these considerations, it is proposed that the thermal conditions of mineralization of the Campbell-Red Lake deposit may be broadly limited in the range from 350 to 550 °C. Using this temperature range and the isochore derived from the lower limit of homogenization temperatures of carbonic inclusions (−2.4 °C), the fluid pressures are estimated to be 2.7–3.6 kbar (Table 2). These pressures are comparable to those estimated from metamorphic mineral assemblages, i.e., 3.8–4.2 kbar estimated by Mathieson and Hodgson (1984), 3–4 kbar by Christie (1986), and <3 kbar by Tarnocai (2000), but are significantly higher than the 1.0–2.2 kbar estimated by Damer (1997). Thompson (2003) noted that the pressure estimation by Damer (1997) is too low from the regional geologic setting consideration and proposed a possible range of pressure from 2 to 4 kbar.

Although it has been shown that the carbonic inclusions in the Red Lake greenstone belt are real records of fluids present during carbonate veining and Au mineralization, it remains a possibility that the carbonic inclusions represent the carbonic phase resulting from phase separation of an initially carbonic-aqueous fluid. The occurrence of aqueous inclusions (although rare) in the vein minerals together with carbonic inclusions is compatible with such a scenario. The question is what kind of composition is required of the initial fluid, given the temperature and pressure conditions discussed above, in order to produce an H_2O-poor, carbonic fluid. To answer this question, a fluid phase separation modeling, using the UCSD-Chemical Geology Group "GeoFluids" program, which is based on the Duan et al. (1995) equation of state for the H_2O–CO_2–NaCl system, is carried out as follows.

The initial fluid is approximated by the H_2O–CO_2–NaCl system, and four different initial compositions are tested, with the mole fractions of H_2O, CO_2, and NaCl from 0.9 to 0.16, 0.07–0.80, and 0.03–0.04, respectively (Fig. 4). The NaCl composition is based on the most frequently recorded values in orogenic Au deposits (Ridley and Diamond, 2000; Fig. 4). Calculations were run for pressures of 2 and 3 kbar and temperatures of 400 and 500 °C to simulate the mineralization conditions, and tests were also made at lower pressure and temperature conditions (1 kbar and 300 °C) for comparison. For each initial composition, it is first tested whether or not phase separation can take place at the given pressure–temperature conditions. If there is phase separation, the vol.%, density, and H_2O–CO_2–NaCl composition of the co-existing liquid and vapor phases at the time of entrapment are calculated (Fig. 4). The vol.% of the vapor phase within the vapor inclusions at 50 °C are also calculated and graphically represented (Fig. 4), in order to provide a visual estimation of what a vapor inclusion resulting from phase separation may look like at room temperature.

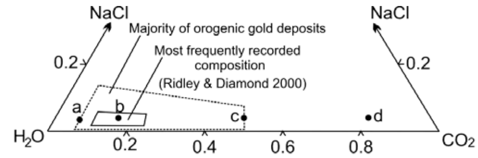

Initial fluid (mole frac.)	At entrapment								Vapor-rich FI at 50°C
	T (−C)	P (Kb)	Phase	vol.%	Density (g/cm³)	Mole fraction H_2O	Mole fraction CO_2	Mole fraction NaCl	
a	300	3	V	22.3	0.968	0.518	0.482	0.000	67%
			L	77.7	1.005	0.965	0.000	0.035	
H_2O = 0.9		2	V	31.3	0.875	0.697	0.303	0.000	51%
CO_2 = 0.07			L	68.7	0.970	0.960	0.000	0.040	
NaCl = 0.03		1	V	29.8	0.718	0.649	0.351	0.000	64%
			L	70.2	0.900	0.960	0.003	0.037	
b	350	3	V	21.1	0.933	0.405	0.594	0.001	77%
			L	78.9	0.992	0.865	0.088	0.047	
H_2O = 0.8		2	V	22.1	0.816	0.472	0.527	0.001	75%
			L	77.9	0.933	0.857	0.096	0.047	
CO_2 = 0.16	300	3	V	46.1	0.984	0.345	0.655	0.000	81%
			L	53.9	1.043	0.946	0.000	0.054	
NaCl = 0.04		2	V	42.2	0.871	0.398	0.602	0.000	79%
			L	57.8	1.002	0.945	0.000	0.055	
		1	V	48.1	0.677	0.435	0.565	0.000	81%
			L	51.9	0.937	0.943	0.001	0.056	
c	500	3	V	87.4	0.845	0.438	0.560	0.002	76%
			L	12.6	1.167	0.671	0.115	0.214	
		2	V	91.8	0.713	0.453	0.546	0.001	79%
			L	8.2	1.220	0.652	0.063	0.285	
		1	V	95.5	0.476	0.467	0.533	0.000	85%
			L	4.5	1.283	0.594	0.031	0.375	
H_2O = 0.48	400	3	V	57.3	0.913	0.332	0.667	0.001	82%
			L	42.7	1.011	0.626	0.295	0.079	
CO_2 = 0.48		2	V	67.5	0.786	0.356	0.643	0.001	83%
			L	32.5	0.955	0.654	0.251	0.095	
		1	V	91.9	0.558	0.422	0.578	0.000	85%
			L	8.1	1.159	0.747	0.031	0.222	
NaCl = 0.04	300	3	V	78.2	0.999	0.224	0.776	0.000	88%
			L	21.8	1.166	0.887	0.000	0.113	
		2	V	79.3	0.881	0.221	0.779	0.000	90%
			L	20.7	1.114	0.888	0.000	0.112	
		1	V	84.0	0.665	0.252	0.748	0.000	91%
			L	16.0	1.057	0.879	0.000	0.121	
d	500	3	V	95.3	0.872	0.144	0.856	0.000	94%
			L	4.7	1.503	0.355	0.102	0.543	
		2	V	96.3	0.735	0.148	0.852	0.000	94%
			L	3.7	1.506	0.325	0.083	0.592	
H_2O = 0.16	400	3	V	94.1	0.937	0.127	0.873	0.000	94%
			L	5.9	1.427	0.477	0.099	0.424	
		2	V	95.2	0.804	0.134	0.866	0.000	95%
			L	4.8	1.428	0.445	0.085	0.470	
CO_2 = 0.80		1	V	96.9	0.569	0.143	0.857	0.000	96%
			L	3.1	1.446	0.381	0.063	0.556	
NaCl = 0.04	300	3	V	95.9	1.033	0.000	1.000	0.000	100%
			L	4.1	1.351	0.799	0.000	0.201	
		2	V	95.0	0.903	0.017	0.983	0.000	99%
			L	5.0	1.325	0.783	0.000	0.217	
		1	V	96.7	0.673	0.043	0.957	0.000	99%
			L	3.3	1.304	0.746	0.000	0.254	

Fig. 4. Simulation of fluid phase separation from an H_2O–CO_2–NaCl parent fluid into a CO_2-enriched vapor and a NaCl-enriched liquid, based on the equations of Duan et al. (1995). The volumetric proportions of the two phases and their compositions are shown for different *T*–*P* conditions. See text for more detailed explanation.

For an initial composition of $H_2O = 0.9$, $CO_2 = 0.07$, and NaCl = 0.03 (point *a*, Fig. 4), phase separation is not possible at temperatures >350 °C. At *T* = 300 °C and *P* = 1, 2, and 3 kbar, phase separation produces 22.3–31.3% vapor and 68.7–77.7% liquid, and the vapor phase contains 0.518–0.697 mole fraction of H_2O, which produces a significant portion of aqueous phase at 50 °C (Fig. 4).

For a fluid of $H_2O = 0.8$, $CO_2 = 0.16$, and NaCl = 0.04 (point *b*, Fig. 4), phase separation is not possible at temperatures > 400 °C. At *T* = 350 °C phase separation does not take place at *P* = 1 kbar, but does so at *P* = 2 and 3 kbar. Phase separation produces 21.1–22.1% vapor and 77.9–78.9% liquid. At *T* = 300 °C, phase separation takes place at P = 1, 2, and 3 kbar, producing 42.2–48.1% vapor and 51.9–57.8% liquid. At both temperatures, the vapor phase contains significant amounts of water (0.345–0.472 mole fraction), yielding an obvious aqueous rim in the vapor inclusions at 50 °C (Fig. 4).

With increasing CO_2 contents in the initial fluid to a composition of H_2O = 0.48, CO_2 = 0.48, and NaCl = 0.04 (point *c*, Fig. 4), phase separation can take place from T = 300 to 500 °C and P = 1–3 kbar. The vapor phase resulting from phase separation takes 57.3–91.9 volume%, and has H_2O contents from 0.221 to 0.467 mol fractions. A rim of aqueous phase in the vapor inclusions can be visible at 50 °C (Fig. 4).

With further increase of CO_2 contents to H_2O = 0.16, CO_2 = 0.80, and NaCl = 0.04 (point *d*, Fig. 4), phase separation can take place from T = 300 to 400 °C and P = 1–3 kbar. At T = 500 °C, phase separation cannot take place for P = 1 kbar, but can for P = 2 and 3 kbar. The vapor phase resulting from phase separation is volumetrically dominant (94.1–96.9%), and the liquid phase is minor (3.1–5.9%). Water contents in the vapor phase range from 0.000 to 0.148 mol fraction, and an aqueous phase rim may be absent or minor in the vapor inclusions at 50 °C (Fig. 4).

The modeling results indicate that although phase separation is generally possible for the H_2O–CO_2–NaCl system and can produce a relatively CO_2-enriched vapor phase, there are important restrictions on the composition of the initial fluid and pressure–temperature conditions in order to produce a H_2O-poor, CO_2-dominated vapor phase. An initially H_2O-rich fluid (cases *a* and *b*, Fig. 4) can only experience phase separation at temperatures below 400 °C, and the vapor phase thus produced contains significant amounts of H_2O. An initial fluid with equal amounts of H_2O and CO_2 (case *c*, Fig. 4) can experience phase separation at the pressure–temperature conditions interpreted for the Campbell-Red Lake deposit, but cannot produce a vapor that is poor in water. It appears that an initially CO_2-dominated fluid, with $X_{CO_2} > 0.8$, is required to produce a H_2O-poor, CO_2-dominated vapor. Two mechanisms have been previously proposed by Crawford and Hollister (1986) to explain the entrapment of CO_2-dominated fluid inclusions without co-existing aqueous inclusions. Firstly, the CO_2-dominated phase can be entrapped as "impurities" as crystals grow (primary inclusions), whereas the aqueous phase that wets the crystal phase may remain outside the advancing crystal front without being entrapped. Secondly, capillary action may "wick" the aqueous phase out of microfractures (due to its low wetting angles), leaving behind the CO_2-dominated phase entrapped as CO_2-dominated inclusions (pseudosecondary and secondary). However, these mechanisms alone cannot explain the rarity of aqueous inclusions, as indicated by the common occurrences of both aqueous and carbonic inclusions in most orogenic Au deposits. The CO_2-dominated nature of the initial fluid and consequently a small proportion (<5%) of aqueous phase being produced from phase separation, coupled with the above two mechanisms, may have been responsible for the rarity of aqueous inclusions in the mineralizing systems in the Red Lake greenstone belt.

5. CO_2 requirement and source constraints

Previous studies of the hydrothermal alterations related to Au mineralization in the Red Lake greenstone belt all indicate that CO_2, S, Au, and K were added from the hydrothermal fluids to the host rocks (Andrews et al., 1986; Parker, 2000), which is similar, but not unique, to most orogenic Au deposits (Groves et al., 2003; Goldfarb et al., 2005; Dubé and Gosselin, 2007). It should be intriguing to calculate how much CO_2 was input to the Red Lake greenstone belt in relation to Au mineralization, and how large a source area is required to produce the amount of CO_2 that passed through the greenstone belt and resulted in the observed carbonate fixation. Because carbonate alteration (and veining) is not evenly distributed in the Red Lake greenstone belt, it is very difficult to make an estimate of the total amount of CO_2 being added to the whole greenstone belt. However, it is possible to have an order-of-magnitude estimate for individual deposits. Since the Campbell-Red Lake deposit is the largest deposit in the region, contributing 840 t out of about 1000 t Au for the greenstone belt, the calculations are focused on this deposit.

Two methods can be used to estimate the amounts of CO_2 being added to a deposit. One is based on estimate of the volume of the mineralized zone (including the non-economic alteration part) and the average CO_2 content, as used by Phillips et al. (1987) for the giant Golden Mile Au deposit, Kalgoorlie, Australia. The other relies on estimation of the amount of fluids passing through the mineralization zone and the deposition efficiency of CO_2, with the amount of fluid being calculated based on the amount of metal deposited and assumptions of metal solubility and deposition efficiency. The second method has large uncertainties associated with it, but it can provide important constraints on Au solubility and the source regions. The calculation results for the Campbell-Red Lake deposit and assumptions associated with them are listed in Table 3 and explained in detail below.

The mineralization + alteration zone of the Campbell-Red Lake deposit is about 2 km long, 250 m wide, and 2 km deep. Carbon dioxide contents range from 28.5 to 42.9 wt.% in ankerite veins (Parker, 2002), 6.5–20.9 in carbonate breccia (Cadieux et al., 2006), and 5.2–13.6 wt.% in the carbonate–biotite alteration envelope (Cadieux et al., 2006) or 7.3–23.6 wt.% in altered ultramafic rocks (Tarnocai, 2000). Other alteration rocks (aluminous alteration and garnet–magnetite alteration), however, contain as little CO_2 as <0.18–3.5 wt.% (Cadieux et al., 2006). Due to lack of systematic chemical analysis across the mineralization + alteration zone, the total amount of CO_2 cannot be determined with certainty. However, based on the rather small number of analyses, it seems an average CO_2 content of 10 wt.% is probably within the order-of-magnitude range. Using this tentative value and a rock density of 2.9 g/cm^3 (as used by Phillips et al., 1987 for Golden Mile), the total amount of CO_2 in the Campbell-Red Lake mineralization zone is 290 Mt (case *a*, Table 3). For comparison, Phillips et al., 1987 used a CO_2 content of 11% for the chlorite zone and 14% for the carbonate zone in their calculation of total CO_2 input in the Lake View mine, which led to an estimation of total CO_2 amount of 340 Mt for the Golden Mile deposit.

The next four cases (cases *b*–*e*, Table 3) are based on the calculation of the amount of fluid flowing through to deposit 840 t Au in the Campbell-Red Lake deposit. Parameters used in the calculations are varied with reference to a Au solubility of 2 μg/L, a Au deposition efficiency of 80%, and a CO_2 deposition efficiency of 10%. The low Au solubility value is chosen for reference based on an estimation by Seward and Barnes (1997) for vein-type Ag–Au deposits (1–10 μg/L) and on measurements of Au in some modern hydrothermal solutions (<0.1–23 μg/L; Simmons and Brown, 2008). The Au and CO_2 deposition efficiency values are considered by Phillips et al. (1987) as "best estimate" for the Golden Mile deposit based on thermodynamic calculations by Neall (1985), which indicate no significant change in the activity of CO_2 and a drop of Au concentration in the solution by more than 90% across alteration zones. X_{CO_2} is assumed to be 0.8 (i.e., 91 wt.% CO_2) based on observations of fluid inclusions and phase separation modeling discussed above.

Assuming a Au solubility value of 2 μg/L, the total amount of mineralizing fluid passing through the Campbell-Red Lake deposit is calculated as $Fluid = \frac{840(t)}{2 \times 10^{-9} \times 80\%} = 5.25 \times 10^{11}(t)$. This amount of fluid contains $5.25 \times 10^{11}(t) \times 91\% = 4.78 \times 10^{11}(t)$ of CO_2. Since the deposition efficiency of CO_2 is 10%, the total amount of CO_2 deposited is $4.78 \times 10^{11}(t) \times 10\% = 4.78 \times 10^{10}(t)$ = 47,800 Mt. This

Table 3
Estimations of the total amount of CO_2 input in the Campbell-Red Lake Au deposit and source requirements.

CO_2 requirement		CO_2 (Mt)	Assumptions	
(a) Total amount of CO_2 based on estimated vein and altered rock volume and average CO_2 content in the Campbell-Red Lake mineralization + alteration zone		290	The mineralization + alteration zone = 2000 m long, 250 m wide, and 2000 m deep; rock density = 2.9 g/cm^3; average CO_2 concentration = 10 wt.%	
Total amount of CO_2 based on total Au input (840 t) and assumptions about Au solubility and deposition efficiency, CO_2 deposition efficiency, and $X_{CO_2} = 0.8$ (~91 wt.%).	(b) Assuming very low Au solubility	47,800	Au solubility = 2 μg/L; Au deposition efficiency = 80%, CO_2 deposition efficiency = 10%	
	(c) Assuming very high Au solubility	478	Au solubility = 200 μg/L; Au deposition efficiency = 80%, CO_2 deposition efficiency = 10%	
	(d) Assuming very low CO_2 deposition efficiency	478	Au solubility = 2 μg/L; Au deposition efficiency = 80%, CO_2 deposition efficiency = 0.1%	
	(e) Moderately high Au solubility and low CO_2 deposition efficiency	478	Au solubility = 20 μg/L; Au deposition efficiency = 80%, CO_2 deposition efficiency = 1%	
Source constraints		Source area (km^2)	Assumptions	Source rock Au (ppb)
Source area for a 5 km thick source region using parameters considered by Phillips et al. (1987) as "best estimate" for Golden Mile, Australia: CO_2 concentration in source rock = 1%; CO_2 extraction efficiency = 60%; Au extraction efficiency = 80%; source rock density = 3 g/cm^3	Case *a* above	32	Total CO_2 flowing through = 2900 Mt; deposition efficiency = 10 wt.%	19.7
	Case *b* above	5275	Total CO_2 flowing through = 478,000 Mt; deposition efficiency = 10 wt.%	0.1
	Case *c* above	53	Total CO_2 flowing through = 4780 Mt; deposition efficiency = 10 wt.%	11.9
	Case *d* above	5275	Total CO_2 flowing through = 478,000 Mt; deposition efficiency = 0.1 wt.%	0.1
	Case *e* above	528	Total CO_2 flowing through = 47,800 Mt; deposition efficiency = 1 wt.%	1.2

amount (case *b*, Table 3) is two orders of magnitude higher than the estimation of case *a*, which is considered to be more plausible. To reduce this large discrepancy, significant changes must be made to case *b*: either the Au solubility is two orders of magnitude higher (i.e., 200 μg/L; case *c*, Table 3), or the CO_2 deposition efficiency is two orders of magnitude lower (i.e., 0.1%; case *d*, Table 3), or a combination of the two (gold solubility = 20 μg/L, CO_2 deposition efficiency = 1%; case *e*, Table 3). In each of these cases, the amount of CO_2 deposited would be 478 Mt, which is within the same order-of-magnitude as case *a*.

The above different scenarios have very different implications on the source regions. Using again the "best estimate" of the source regions by Phillips et al., 1987: CO_2 concentration in source rock = 1%; CO_2 extraction efficiency = 60%; source rock density = 3 g/cm^3, the area of a 5 km thick source region can be calculated for the different cases (Table 3). In case *a*, the source area is estimated to be 32 km^2, which is comparable to that in the Golden Mile deposit, Kalgoorlie (38 km^2, Phillips et al., 1987). Assuming a Au extraction efficiency of 80% as Phillips et al. (1987), the Au concentration in the source rocks can be calculated to be 19.7 ppb (Table 3). In cases *b* and *d*, however, an unrealistically large source area of 5275 km^2 would be required, in order to account for the very large amount of fluid involved (478,000 Mt; Table 3). Consequently, the requirement of Au concentration in the source rocks is only 0.1 ppb (Table 3). On the other hand, in case *c*, where high solubility of Au (200 μg/L) is assumed, a source area of 53 km^2 is required because only 4780 Mt of fluid is needed, and the Au concentration in the source rocks is calculated to be 11.9 ppb (Table 3). In case *e* (with a moderately high Au solubility of 20 μg/L), the source area required is 528 km^2, and the Au content in the source rocks is 1.2 ppb (Table 3). It appears that Au solubility significantly higher than the 2 μg/L level is required in order to deposit the total amount of Au (840 t) without having to extract too much fluid, which would require an unrealistically large source region in order to provide the amount of CO_2. Assuming a higher CO_2 content (>1 wt.%) in the source region can ease the problem only slightly, and is not supported by a belt-scale petrochemical analysis (Parker, 2002), which indicates an average of 1.95 wt.% CO_2, with the majority of analysis being less than 0.5 wt.%.

In summary, a total of 290 Mt of CO_2 is estimated to have been deposited in the Campbell-Red Lake mineralization zone based on a speculative average CO_2 content of 10 wt.% and a volume of 250 m × 2000 m × 2000 m. The amount of fluid required to deposit this amount of CO_2 is constrained by the total amount of Au deposited (840 t), Au solubility, Au deposition efficiency, CO_2 deposition efficiency, and source region limitation. It is shown that under the assumption of a Au solubility of 2 μg/L and the best estimate of conditions of Phillips et al. (1987) (Au deposition efficiency = 80%; CO_2 deposition efficiency = 10%), the amount of CO_2 deposited would be two orders of magnitude higher than the above estimation (i.e., 290 Mt CO_2). If the CO_2 deposition efficiency is reduced to 0.1% instead of 10%, the amount of CO_2 deposited would be comparable to the first estimation, but the amount of fluid involved would be two orders of magnitude higher than could be realistically provided by a reasonable volume of source region. The very large source rock volume also implies that the Au concentration in the source rocks is extremely low (0.1 ppb, Table 3), even lower than the Clarke value (4 ppb; Mason and Moore, 1982). To reconcile the discrepancy resulting from calculations based on Au transport and deposition and source region constraints, a Au solubility significantly higher than usually assumed (a few μg/L), e.g., 200 μg/L, is required.

6. Discussion

The relationship between the CO_2-dominated mineralizing fluids and alterations (especially those involving hydrous minerals such as biotite, sericite, and chlorite) needs to be discussed. The CO_2-dominated nature of the fluids may be reflected by X_{CO_2} values calculated from alteration mineral assemblages, which are broadly contemporaneous with peak metamorphism. X_{CO_2} values from 0.45 to 0.85 have been obtained by Damer (1997) for the Red Lake mine. These values are significantly higher than those for most orogenic Au deposits (0.05–0.25; McCuaig and Kerrich, 1998), and are consistent with the unusually CO_2-dominated nature of fluids as indicated by fluid inclusions. However, the X_{CO_2} values calculated from mineral assemblages are not necessarily the same as the fluids passing through the main conduits (fractures now filled by veins). Tarnocai (2000) noticed an increase of X_{CO_2} from 0.025 in rocks distal to auriferous veins to 0.45 adjacent to the veins in the Campbell mine. It is likely that the CO_2-dominated fluids, which were probably advected from a deeper part of the crust, are mainly confined in fluid conduits, whereas H_2O-dominated fluids, which may have been derived from the ambient environment, become increasingly important away from the conduits (Fig. 5). Therefore, the CO_2-dominated nature of the mineralizing fluids is not inconsistent with the development of hydrous alterations in the host rocks. Such a profile of decreasing X_{CO_2} values away from the conduits may be present both in the proximal ferroan dolomite zones and in the distal calcite zones.

Helium isotopes of fluid inclusions from the Campbell-Red Lake deposit indicate that the fluids were derived from a crustal source (Chi et al., 2006). It is known that the CO_2 contents of metamorphic fluids generally increase with metamorphic grades (Crawford, 1981; Crawford and Hollister, 1986) and CO_2-dominated fluid inclusions are commonly found in granulite facies rocks and associated granitoids (Touret, 1981; Santosh et al., 2005). It is proposed here that the CO_2-dominated fluids in the Red Lake greenstone belt were derived from granulite facies source rocks, and were expelled upward along major structures, passing through the amphibole facies rocks, where the ambient fluids have moderate X_{CO_2}, and then to the greenschist facies rocks with low X_{CO_2} (Fig. 5). A gradient of X_{CO_2} may be established across the conduits as the CO_2-dominated fluids passed through host rocks with lower X_{CO_2} values (Fig. 5). The dominance of CO_2-dominated fluids within the conduits may have lasted longer in major hydrothermal-deformation corridors such as the Red Lake Mine trend hosting the Campbell-Red Lake and Cochenour deposits, and was relatively short-lived in less deformed zones such as the Redcon prospect and the Sandy Bay – Woodland Cemetery outcrop, where more aqueous fluid inclusions are found as secondary inclusions, indicating incursion of the ambient H_2O-dominated fluids.

Because the solubilities of carbonate minerals, unlike most other minerals, increase with decreasing temperature, the precipitation of carbonate minerals cannot have been caused by cooling of hydrothermal fluids (Kerrich and Fyfe, 1981). Two mechanisms may be envisaged to explain the deposition of large amounts of carbonate in the veins. The first one calls for the mixing of a H_2O-poor, CO_2-dominated fluid with an aqueous fluid containing Ca^{2+}, Fe^{2+} and Mg^{2+}, and the reactions involved are as follows:

$$CO_2(g) + H_2O \Longleftrightarrow H_2CO_3 \quad (1)$$

$$H_2CO_3 \Longleftrightarrow HCO_3^- + H^+ \quad (2)$$

$$HCO_3^- \Longleftrightarrow CO_3^{2-} + H^+ \quad (3)$$

$$Ca^{2+} + CO_3^{2-} \Longleftrightarrow CaCO_3 \quad (4)$$

Whether calcite or ankerite was precipitated depends on the contents of Ca^{2+}, Fe^{2+}, and Mg^{2+} in the aqueous solution, which may have been locally derived from the host rocks (Kerrich and Fyfe, 1981). Continuous input of CO_2, however, is unfavorable for carbonate precipitation because it will cause a pH decrease through reactions 1–3 above. In order for carbonates to continue

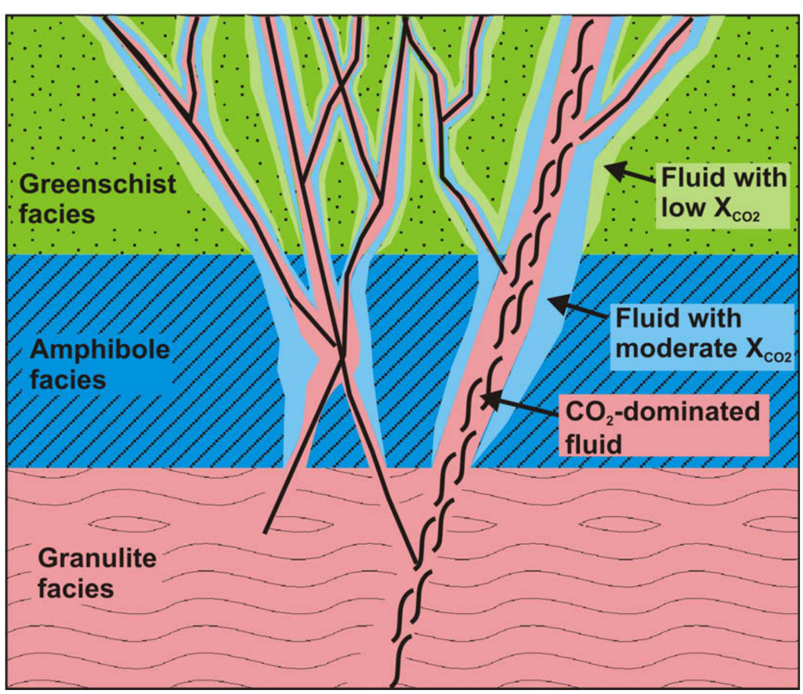

Fig. 5. A sketch cross-section showing the distribution of different kinds of fluids in different crustal levels. CO_2-dominated fluids were derived from the granulite facies, and were channeled along major structures and then delivered to lower-order fractures. Fluids in the amphibole facies have moderately low X_{CO_2}, whereas those in the greenschist facies are dominated by H_2O. Fluids of intermediate X_{CO_2} values resulted from mixing between CO_2-dominated fluids and ambient fluids of lower X_{CO_2} values. Note the X_{CO_2} profile shown in this figure may be present both in the proximal ferroan dolomite zones and the distal calcite zones.

precipitation, H^+ must be consumed by some water-rock interactions. Such reactions are recorded by potassic (sericite/muscovite or biotite) alteration accompanying carbonatization (Parker, 2000).

The second mechanism of carbonate precipitation is by phase separation of a fluid initially containing CO_2, Ca^{2+}, Fe^{2+} and Mg^{2+}. The reaction involved may be expressed as

$$CaCO_3 + H_2O + CO_2(g) \Longleftrightarrow Ca^{2+} + 2HCO_3^- \quad (5)$$

A loss of CO_2 through phase separation will cause the reaction to proceed toward the left and precipitation of calcite. It is possible that both fluid mixing and phase separation were involved in the precipitation of carbonates in the veins.

Although Au mineralization is spatially associated with carbonate veining (the proximal ferroan dolomite zone of Parker, 2000), it has been shown that Au deposition is closely associated with silica and sulfides (especially arsenopyrite) which, at least in part, replace carbonates. However, this does not mean that all Au mineralization postdates carbonate veining, because some carbonate ± quartz veins cut Au mineralized zones (Dubé et al., 2002). The spatial association between carbonate and Au mineralization has been related to the increased competency of the country rocks due to carbonatization that enhances brittle fracture and Au veining (Goldfarb et al., 2005). It may also be due to the common structural control of the fluid causing carbonate veining and that responsible for Au deposition, even if the two fluids are not genetically related. However, based on similarity of fluid inclusions in ankerite and Au-associated quartz, it is likely that the fluids that deposited Au, silica and sulfides are part of the same evolving (or protracted) hydrothermal system responsible for precipitating the carbonate ± quartz veins. The reason that the bulk of the carbonate deposition predates silicification and Au deposition is probably that carbonate becomes oversaturated at higher temperatures than Au and silica. As temperature continues to decrease following carbonate deposition, Au and silica became oversaturated and were deposited, whereas carbonates were locally dissolved due to their increased solubility caused by decreased temperature. This may explain the partial replacement of carbonate ± quartz veins by silica, sulfides and Au.

The association of CO_2-dominated fluid inclusions and Au mineralization in the Red Lake greenstone belt implies that Au can be transported by H_2O-poor, CO_2-dominated fluids. Carbon dioxide by itself is not an important agent for Au transport because it is a non-polar molecule. Trace amounts of H_2S were detected by laser-Raman on individual inclusions (<0.1 mol%) and by gas chromatography on bulk inclusions (not quantified) in the Campbell-Red Lake deposit (Chi et al., 2006), and it has been postulated that Au may have been transported as HS^- complexing or as H_2S-solvated species having the stoichiometry $Au.n(H_2S)^{gas}$ (Chi et al., 2005, 2006). Zezin et al. (2007) have shown that gold can be dissolved in H_2S gas as $AuS.(H_2S)n$ or $AuHS.(H_2S)n$. Loucks and Mavrogenes (1999) demonstrated experimentally that at high temperature (550–725 °C) and pressure (1–4 kbar) conditions, Au is transported as $AuHS(H_2S)_3^0$, and therefore dissolved H_2S gas that is ineffective in metal complexing at low pressures is highly effective at high pressures. Gold solubility at these high pressure-high temperature conditions can be extremely high, up to several hundreds of mg/L (Loucks and Mavrogenes, 1999). The capacity of CO_2-rich fluids to transport metals has also been demonstrated by the presence of chalcopyrite daughter mineral in CO_2-rich fluid inclusions (Lai and Chi, 2007). The calculations on CO_2 requirement and source constraints for the Campbell-Red Lake deposit, as shown above, suggest that Au solubility was likely in the order of several hundreds of μg/L, which appears unusually high compared to the common assumption of only a few μg/L of Au in ore-forming fluids (Seward and Barnes, 1997) but is possible in light of Loucks and Mavrogenes (1999) experiments. The high Au solubility may also explain why the Campbell-Red Lake deposit has such a high-grade of Au (average 21 g/t for the whole deposit, and average 80.6 g/t for the Goldcorp High-Grade zone).

The well developed colloform–crustiform structures in the carbonate ± quartz veins have been interpreted as indicating epithermal mineralization environments (Penczak and Mason, 1997, 1999) or a relatively shallow (epizonal) crustal level (possibly 2–5 km from surface) similar to the high-level orogenic systems at Wiluna, Australia (Dubé et al., 2002, 2004). However, crosscutting relationships and isotopic dating suggest that the main phase Au mineralization, and at least part of the carbonate veining, occurred broadly during regional metamorphism, which took place at pressures from 2 to 4 kbar, corresponding to depths of 7–14 km (Thompson, 2003). Carbonic fluid inclusions with very low homogenization temperatures (as low as −12.6 °C, Table 1) in ankerite are consistent with the interpreted large pressures and depths. It is speculated here that the apparent conflict between colloform–crustiform structures and deep formation environments indicated by fluid inclusions may be related to the unusually high CO_2 contents in the hydrothermal fluids. It is known that CO_2-dominated fluids have high wetting angles (Watson and Brenan, 1987), which prevent interconnection of fluid phase in the host rocks and thus enhance the brittle properties of the rocks. The development of colloform–crustiform structures may also be related to extremely high fluid pressures which helped create high dilation rates favorable for forming open-space filling structures (Dubé et al., 2002).

7. Conclusions

In conclusion, fluid inclusion studies indicate that CO_2-dominated fluids were involved in carbonate ± quartz vein formation and Au mineralization not only in the Campbell-Red Lake Au deposit, but also in small Au occurrences and non-mineralized veins in the Red Lake greenstone belt. Fluid phase separation modeling indicates that the CO_2-dominated fluids likely have X_{CO_2} values > 0.8. Hydrothermal mineral assemblages in the host rocks indicate X_{CO_2} values as high as 0.45–0.85, indirectly supporting the CO_2-dominated nature of the hydrothermal fluids. However, X_{CO_2} values in the host rocks are generally lower than in the veins and have the tendency to decrease away from the veins. This indicates that the CO_2-dominated fluids are mainly confined in fractures (veins), which may migrated laterally into the host rocks and mix with H_2O-dominated fluids, resulting in intermediate X_{CO_2} values. The CO_2-dominated fluids may have been derived from granulite facies in deeper parts of the crust, whereas H_2O-dominated fluids were dominant in the ambient host rocks of amphibole and greenschist facies. Carbonate deposition may be related to fluid phase separation or mixing between CO_2-dominated fluids and H_2O-dominated fluids carrying Ca^{2+}, Mg^{2+} and Fe^{2+}. The fluids depositing carbonates were probably part of the same evolving and protracted large scale hydrothermal system precipitating SiO_2 and Au: the bulk of the carbonates precipitated first at relatively high temperatures, became partly dissolved at lower temperatures (due to increased solubility), when SiO_2 and Au were deposited and partly replaced carbonates. Mass balance calculations indicate that in order to deposit the speculative amount of CO_2 (290 Mt) and the total amount of Au (840 t) in the Campbell-Red Lake deposit from the same evolving large scale hydrothermal fluid, the Au solubility in the fluid must be around 200 μg/L, which is two orders of magnitude higher than the usually assumed values of a few μg/L. The high Au contents of the CO_2-dominated fluids may have been responsible for the high-grades of Au in the Campbell-Red Lake deposit.

Acknowledgements

This study is supported by an NSERC-Discovery grant to Chi. We would like to thank Andreas Lichtblau and Carmen Storey of Ontario Geological Survey, Kenneth Williamson and Paul Barc of Goldcorp, Farhad Bouzari of the University of British Columbia, and Mary Louise Hill of Lakehead University for their help in field work and for helpful discussion. Critical and constructive reviews by Jayanta Guha and Gema Olivo and an anonymous reviewer have helped improve the manuscript.

References

Andrews, A.J., Hugon, H., Durocher, M., Corfu, F., Lavigne, M., 1986. The anatomy of a gold-bearing greenstone belt: Red Lake, northwestern Ontario, Canada. In: MacDonald, A.J. (Ed.), Proc. Gold'86 Symp. Toronto, pp. 3–22.

Baker, T., 2002. Emplacement depth and carbon dioxide-rich fluid inclusions in intrusion-related gold deposits. Econ. Geol. 97, 1111–1118.

Bakker, R.J., Jansen, J.B.H., 1994. A mechanism for preferential H_2O leakage from fluid inclusion in quartz, based on TEM observations. Contrib. Mineral. Petrol. 116, 7–20.

Cadieux, A.-M., Dubé, B., Williamson, K., Malo, M., Twomey, T., 2006. Characterization of hydrothermal alterations at the Red Lake mine, northwestern Ontario. Geol. Surv. Can., Curr. Res. C2.

Chi, G., Dubé, B., Williamson, K., 2002. Preliminary fluid-inclusion microthermometry study of fluid evolution and temperature–pressure conditions in the goldcorp high-grade zone, Red Lake mine, Ontario. Geol. Surv. Can., Curr. Res. C27.

Chi, G., Dubé, B., Williamson, K., 2003. Fluid evolution and pressure regimes in the Red Lake Mine Trend: fluid-inclusion evidence for a protracted, highly dynamic hydrothermal system. Geol. Surv. Can., Curr. Res. C28.

Chi, G., Dube, B., Williamson, K., Williams-Jones, A.E., 2006. Formation of the Campbell-Red Lake gold deposit by H_2O-poor, CO_2-dominated fluids. Mineral. Dep. 40, 726–741.

Chi, G., Williams-Jones, A.E., Dubé, B., Williamson, K., 2005. Carbonic vapor-dominated fluid systems in orogenic-type Au deposits. Geochim. Cosmochim. Acta 69, A738.

Christie, B.J., 1986. Alteration and gold mineralization associated with a sheeted veinlet zone at the Campbell Red Lake mine. Unpublished M.Sc. Thesis, Queen's Univ., Kingston, Canada.

Corfu, F., Andrews, A.J., 1987. Geochronological constraints on the timing of magmatism, deformation, and gold mineralization in the Red Lake greenstone belt, northwestern Ontario. Can. J. Earth Sci. 24, 1302–1320.

Crawford, M.L., 1981. Fluid inclusions in metamorphic rocks – low and medium grade. In: Hollister, L.S., Crawford, M.L. (Eds.), Fluid Inclusions Applications to Petrology. Mineral. Assoc. Can. Short Course 6, pp. 157–181.

Crawford, M.L., Hollister, L.S., 1986. Metamorphic fluids: the evidence from fluid inclusions. In: Walther, J.V., Wood, B.J. (Eds.), Fluid–Rock Interactions during Metamorphism Advances in Physical Geochemistry, vol. 5. Springer-Verlag, New York, pp. 1–35.

Damer, D.C., 1997. Metamorphism of hydrothermal alteration at the Red Lake Mine, Balmertown, Ontario. Unpublished Master Thesis, Queen's Univ., Kingston, Canada.

Duan, Z., Moller, N., Weare, J.H., 1995. Equation of state for the $NaCl–H_2O–CO_2$ system: prediction of phase equilibria and volumetric properties. Geochim. Cosmochim. Acta 59, 2869–2882.

Dubé, B., Gosselin, P., 2007. Greenstone-hosted quartz–carbonate vein deposits. In: Goodfellow, W.D. (Ed.), Mineral Deposits of Canada. Geol. Assoc. Can., MDD Special Publication No. 5, pp. 49–73.

Dubé, B., Balmer, W., Sanborn-Barrie, M., Skulski, T., Parker, J., 2000. A preliminary report on amphibolite-facies, disseminated-replacement-style mineralization at the Madsen gold mine, Red Lake, Ontario. Geol. Surv. Can., Curr. Res. C17.

Dubé, B., Williamson, K., Malo, M., 2001. Preliminary report on the geology and controlling parameters of the Goldcorp Inc. High-grade Zone, Red Lake Mine, Ontario. Geol. Surv. Can., Curr. Res. C18.

Dubé, B., Williamson, K., Malo, M., 2002. Geology of the Goldcorp Inc. High Grade zone, Red Lake mine, Ontario: an update. Geol. Surv. Can., Curr. Res. C26, 13.

Dubé, B., Williamson, K., Malo, M., 2003. Gold mineralization within the Red Lake mine trend: example from the Cochenour–Willans mine area, Red Lake, Ontario, with new key information from the Red Lake mine and potential analogy with the Timmins camp. Geol. Surv. Can., Curr. Res. C21.

Dubé, B., Williamson, K., McNicoll, V., Malo, M., Skulski, T., Twomey, T., Sanborn-Barrie, M., 2004. Timing of gold mineralization in the Red Lake gold camp, northwestern Ontario, Canada: new constraints from U–Pb geochronology at the Goldcorp High-Grade zone, Red Lake mine and at the Madsen mine. Econ. Geol. 99, 1611–1641.

Garba, I., Akande, S.O., 1992. The origin and significance of non-aqueous CO_2 fluid inclusions in the auriferous veins of Bin Yauri, northwestern Nigeria. Mineral. Dep. 27, 249–255.

Goldfarb, R.J., Baker, T., Dubé, B., Groves, D.I., Hart, C.J.R., Gosselin, P., 2005. Distribution, character, and genesis of gold deposits in metamorphic terranes. In: Hedenquist, J.W., Thompson, J.F.H., Goldfarb, R.J., Richards, J.P. (Eds.), Economic Geology One Hundredth Anniversary Volume, pp. 407–450.

Groves, D.I., Goldfarb, R.J., Gebre-Mariam, M., Hagemann, S.G., Robert, F., 1998. Orogenic gold deposits: a proposed classification in the context of their crustal distribution and relationship to other gold deposit types. Ore Geol. Rev. 13, 7–27.

Groves, D.I., Goldfarb, R.J., Robert, F., Hart, C.J.R., 2003. Gold deposits in metamorphic belts: overview of current understanding, outstanding problems, future research, and exploration significance. Econ. Geol. 98, 1–30.

Guha, J., Lu, H.-Z., Dubé, B., Robert, F., Gagnon, M., 1991. Fluid characteristics of vein and altered wall rock in Archean mesothermal gold deposits. Econ. Geol. 86, 667–684.

Hollister, L.S., 1988. On the origin of CO_2-rich fluid inclusions in migmatites. J. Metamorph. Geol. 6, 467–474.

Hollister, L.S., 1990. Enrichment of CO_2 in fluid inclusions in quartz by removal of H_2O during crystal–plastic deformation. J. Struct. Geol. 12, 895–901.

Johnson, E.L., Hollister, L.S., 1995. Syndeformational fluid trapping in quartz: determining the pressure–temperature conditions of deformation from fluid inclusions and the formation of pure CO_2 fluid inclusions during grain boundary migration. J. Metamorph. Geol. 13, 239–249.

Kerrich, R., Fyfe, W.S., 1981. The gold–carbonate association: source of CO_2, and CO_2 fixation reactions in Archean lode deposits. Chem. Geol. 33, 265–294.

Klemd, R., 1998. Comment on the paper by Schmidt Mumm et al. High CO_2 content of fluid inclusions in gold mineralizations in the Ashanti Belt Ghana: a new category of ore forming fluids? (Mineral Depos 32: 107–118, 1997). Mineral. Dep. 33, 317–319.

Lai, J., Chi, G., 2007. CO_2-rich fluid inclusions with chalcopyrite daughter mineral from the Fenghuangshan Cu–Fe–Au deposit, China: implications for metal transport in vapor. Mineral. Dep. 42, 293–299.

Lang, J.R., Baker, T., 2001. Intrusion-related gold systems: the present level of understanding. Mineral. Dep. 36, 477–489.

Lichtblau, A., Storey, C., 2005. Field Trip Through the Central Red Lake Gold Camp. Ministry of Northern Development and Mines, Ontario Geological Survey.

Loucks, R.R., Mavrogenes, J.A., 1999. Gold solubility in supercritical hydrothermal brines measured in synthetic fluid inclusions. Science 284, 2159–2163.

MacGeehan, P., Hodgson, C.J., 1982. Environments of gold mineralization in the Campbell Red lake and Dickenson mines, Red Lake district, Ontario. In: Hodder, R.W. (Ed.), Geology of Canadian Gold Deposits, vol. 24. Canadian Institute of Mining and Metallurgy, pp. 184–207.

MacGeehan, P.J., Sanders, T., Hodgson, C.J., 1982. Meter-wide veins and a kilometer-wide anomaly: wall-rock alteration at the Campbell Red Lake and Dickenson gold mines, Red Lake district, Ontario. Can. Min. Metall. Bull. 75, 90–102.

Mason, B., Moore, C.B., 1982. Principles of Geochemistry, fourth ed. John Wiley & Sons, New York.

Mathieson, N.A., Hodgson, C.J., 1984. Alteration, mineralization, and metamorphism in the area of East South "C" ore zone, 24th level of the Dickenson mine, Red Lake, northwestern Ontario. Can. J. Earth Sci. 21, 35–52.

McCuaig, T.C., Kerrich, R., 1998. P-T-t-deformation-fluid characteristics of lode gold deposits: evidence from alteration systematics. Ore Geol. Rev. 12, 381–453.

Menard, T., Pattison, D., 1998. Correlation of multiple alteration events with successive tectonic and metamorphic events in the Red Lake greenstone belt, northwestern Ontario: 4th Western Superior Transect Annual Workshop, University of British Columbia, Vancouver, Lithoprobe Report 65, pp. 63–69.

Menard, T., Pettigrew, N., Spray, J., 1999. A joint industry-Lithoprobe project on the tectonic history of gold deposits in the Red Lake greenstone belt, Red Lake, Ontario, 2740-2700 March 5th Western Superior Transect Annual Workshop, University of British Columbia, Vancouver, Lithoprobe Report 70, pp. 97–103.

Mikucki, E.J., Ridley, J.R., 1993. The hydrothermal fluid of Archean lode-gold deposits at different metamorphic grades: compositional constraints from ore and wallrock alteration assemblages. Mineral. Dep. 28, 469–481.

Neall, F.B., 1985. Application of thermodynamics to the study of two Archean hydrothermal gold deposits in Western Australia. Ph.D. Thesis, Univ. Western Australia, Nedlands, Australia.

Parker, J.R., 2000. Gold mineralization and wall rock alteration in the Red Lake greenstone belt: a regional perspective. Summary of Field Work and Other Activities, Ontario Geol. Surv. Open File Report 6032, pp. 22-1–22-28.

Parker, J.R., 2002. Lithogeochemical data from the Red Lake greenstone belt, northwestern Ontario. Ontario Geol. Surv., Misc. Release-Data MRD, 113.

Penczak, R., Mason, R., 1997. Metamorphosed Archean epithermal Au–As–Sb–Zn–(Hg) vein mineralization at the Campbell Mine, Northwestern Ontario. Econ. Geol. 92, 696–719.

Penczak, R., Mason, R., 1999. Characteristics and origin of Archean premetamorphic hydrothermal alteration at the Campbell gold mine, northwestern Ontario, Canada. Econ. Geol. 94, 507–528.

Percival, J.A., Sanborn-Barrie, M., Skulski, T., Stott, G.M., Helmstead, H., White, D.J., 2006. Tectonic evolution of the western superior province from NATMAP and lithoprobe studies. Can. J. Earth Sci. 43, 1085–1117.

Phillips, G.N., Groves, D.I., Brown, I.J., 1987. Source requirements for the golden mile, Kalgoorlie: significance to the metamorphic replacement model for Archean gold deposits. Can. J. Earth Sci. 24, 1643–1651.

Poulsen, K.H., Robert, F., Dubé, B., 2000. Geological classification of Canadian gold deposits. Geol. Surv. Can. Bull., 540.

Ridley, J.R., Diamond, L.W., 2000. Fluid chemistry of orogenic lode gold deposits and implications for genetic models. In: Hagemann, S.G., Brown, P.E. (Eds), Gold in 2000. Reviews in Economic Geology 13, pp. 146–162.

Robert, F., Kelly, W.C., 1987. Ore-forming fluids in Archean gold-bearing quartz veins at Sigma mine, Abitibi greenstone belt, Quebec, Canada. Econ. Geol. 82, 1464–1482.
Sanborn-Barrie, M., Skulski, T., Parker, J.R., 2004. Geology, Red Lake greenstone belt, western Superior Province, Ontario. Geol. Surv. Canada, Open File 4594. 1:50,000 scale color map.
Santosh, M., Tanaka, K., Yoshimura, Y., 2005. Carbonic fluid inclusions in ultrahigh-temperature granitoids from southern India. C.R. Geosci. 337, 327–335.
Schmidt Mumm, A., Oberthür, T., Vetter, U., Blenkinsop, T.G., 1997. High CO_2 content of fluid inclusions in gold mineralizations in the Ashanti Belt, Ghana: a new category of ore forming fluids? Mineral. Dep. 32, 107–118.
Schmidt Mumm, A., Oberthür, T., Vetter, U., Blenkinsop, T.G., 1998. High CO_2 content of fluid inclusions in gold mineralizations in the Ashanti Belt, Ghana: a new category of ore forming fluids? – a reply. Mineral. Dep. 33, 320–322.
Seward, T.M., Barnes, H.L., 1997. Metal transport by hydrothermal ore fluids. In: Barnes, H.L. (Ed.), Geochemistry of Hydrothermal Ore Deposits, third ed. John Wiley and Sons, New York, pp. 435–486.
Simmons, S.F., Brown, K.L., 2008. Precious metals in modern hydrothermal solutions and implications for the formation of epithermal ore deposits. SEG Newslett. 72, 1–12.
Tarnocai, C., 2000. Archean gold mineralization at the Campbell mine, eastern Red Lake greenstone belt, western Superior Province of Canada. Ph.D. Thesis, Univ. Ottawa.
Tarnocai, C.A., Hattori, K., Cabri, L.J., 1997. "Invisible" gold in sulfides from the Campbell mine, Red Lake greenstone belt, Ontario: evidence for mineralization during the peak of metamorphism. Can. Mineral. 35, 805–815.
Thompson, P.H., 2003. Toward a new metamorphic framework for gold exploration in the Red Lake greenstone belt. Ontario Geol. Surv. Open File report 6122.
Touret, J.L.R., 1981. Fluid inclusions in High Grade metamorphic rocks. In: Hollister, L.S., Crawford, M.L. (Eds.), Fluid Inclusions Applications to Petrology, vol. 6. Mineral. Assoc. Can. Short Course, pp. 182–208.
Twomey, T., McGibbon, S., 2001. The geological setting and estimation of gold grade of the Highgrade Zone, Red Lake Mine, Goldcorp Inc. Explor. Mining Geol. 10, 19–34.
Watson, E.B., Brenan, J.M., 1987. Fluids in the lithosphere, 1. Experimentally-determined wetting characteristics of CO_2–H_2O fluids and their implications for fluid transport, host-rock physical properties, and fluid inclusion formation. Earth Planet. Sci. Lett. 85, 497–515.
Xavier, R.P., Foster, R.P., 1999. Fluid evolution and chemical controls in the Fazenda Maria Pretta (FMP) gold deposit, Rio Itapicuru greenstone belt, Bahia, Brazil. Chem. Geol. 154, 133–154.
Zezin, D.Y., Migdisov, A.A., Williams-Jones, A.E., 2007. The solubility of gold in hydrogen sulfide gas: an experimental study. Geochim. Cosmochim. Acta 71, 3070–3081.